nature physics

LETTERS

PUBLISHED ONLINE: 1 AUGUST 2010 | DOI: 10.1038/NPHYS1733

Selective darkening of degenerate transitions demonstrated with two superconducting quantum bits

P. C. de Groot[1]*, J. Lisenfeld[1,2], R. N. Schouten[1], S. Ashhab[3,4], A. Lupaşcu[5], C. J. P. M. Harmans[1] and J. E. Mooij[1]

Controlled manipulation of quantum states is central to studying natural and artificial quantum systems. If a quantum system consists of interacting subunits, the nature of the coupling may lead to quantum levels with degenerate energy differences. This degeneracy makes frequency-selective quantum operations impossible. For the prominent group of transversely coupled two-level systems, that is, qubits, we introduce a method to selectively suppress one transition of a degenerate pair while coherently exciting the other, effectively creating artificial selection rules. It requires driving two qubits simultaneously with the same frequency and specified relative amplitude and phase. We demonstrate our method on a pair of superconducting flux qubits[1]. It can directly be applied to the other superconducting qubits[2–6], and to any other qubit type that allows for individual driving. Our results provide a single-pulse controlled-NOT gate for the class of transversely coupled qubits.

In coupling two qubits one can distinguish interactions that are oriented either along or perpendicular to the eigenstates of the qubits. Although in both cases the resulting two-qubit energy-level spectrum reflects the coupling strength, the response to a change of the state of a qubit differs greatly. With longitudinal coupling the state of one qubit affects the energy splitting of the other qubit. Although this spectroscopic shift enables simple resonant driving for all operations[7,8], in practice it requires refocusing schemes to compensate for the continuously evolving phases[9]. In contrast, for transverse coupling the energy splitting of one qubit does not depend on the state of the other qubit. This last case is appealing, as in the absence of driving the system acts as a set of uncoupled qubits, and the coupling is effectively switched on when a.c. driving is applied[10]. The price to pay for the advantage of transverse coupling is obvious; the degeneracy prohibits schemes for selective excitation that rely on a frequency splitting. Previous experiments used either extra coupling elements[11], extra modes[12] or shifted levels into and out of resonance by d.c. (ref. 13) or strong a.c. fields[14,15]. Note that level shifting can imply passing through conditions of low coherence[16], or passing resonances with other qubits. In contrast, our method works for simple direct coupling as well as for systems with extra coupling elements, such as harmonic oscillators, as long as the effective coupling is transverse. It uses only a single pulse of a single frequency and does not require (dynamical) shifting of the levels.

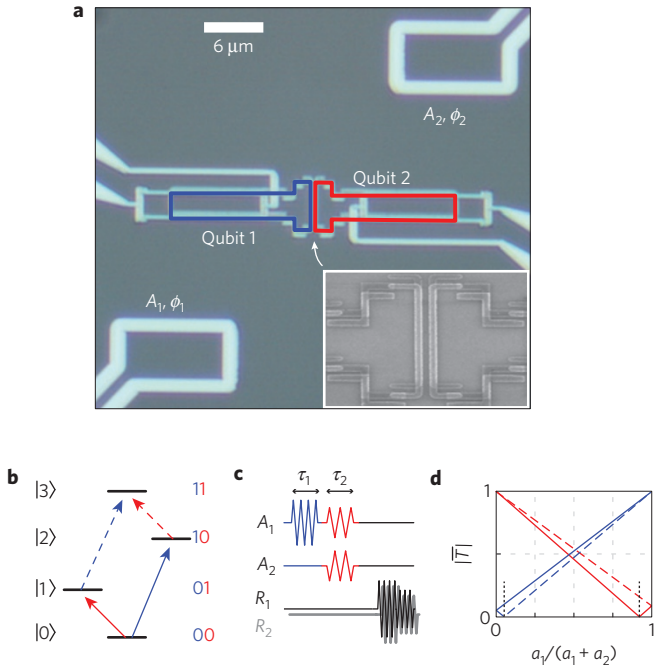

Figure 1 | Coupled qubit system and transitions. a, Optical micrograph of the sample, showing two flux qubits coloured in blue and red. The inset shows part of each qubit loop, both containing four Josephson tunnel junctions. Overlapping the qubit loops, in light grey, are the qubit-state detectors based on superconducting quantum interference devices. In the top right and bottom left are the two antennas from which the qubits are driven. **b**, Energy-level diagram of the coupled qubit system. Arrows of the same colour indicate transitions of the same qubit and are degenerate in frequency. **c**, Pulse sequence used for the coherent excitation of the qubits. The first pulse is resonant with qubit 1. The second pulse, applied from both antennas simultaneously with independent amplitudes and phases, is resonant with qubit 2. After the second pulse the state of both qubits is read out. **d**, The normalized transition strengths of the four transitions in **b** as a function of the net driving amplitudes $a_1/(a_1+a_2)$ for $\varphi_2-\varphi_1=0$. For $\varphi_2-\varphi_1=\pi$ the dashed and solid lines are interchanged. The black dotted lines indicate the locations of the darkened transitions.

[1]Kavli Institute of Nanoscience, Delft University of Technology, PO Box 5046, 2600 GA Delft, The Netherlands, [2]Physikalisches Institut and DFG Center for Functional Nanostructures (CFN), Karlsruhe Institute of Technology, D-76131 Karlsruhe, Germany, [3]Advanced Science Institute, The Institute of Physical and Chemical Research (RIKEN), Wako-shi, Saitama 351-0198, Japan, [4]Department of Physics, University of Michigan, Ann Arbor, Michigan 48109-1040, USA, [5]Institute for Quantum Computing, University of Waterloo, N2L 5G7 Waterloo, Canada. *e-mail: p.c.degroot@tudelft.nl.

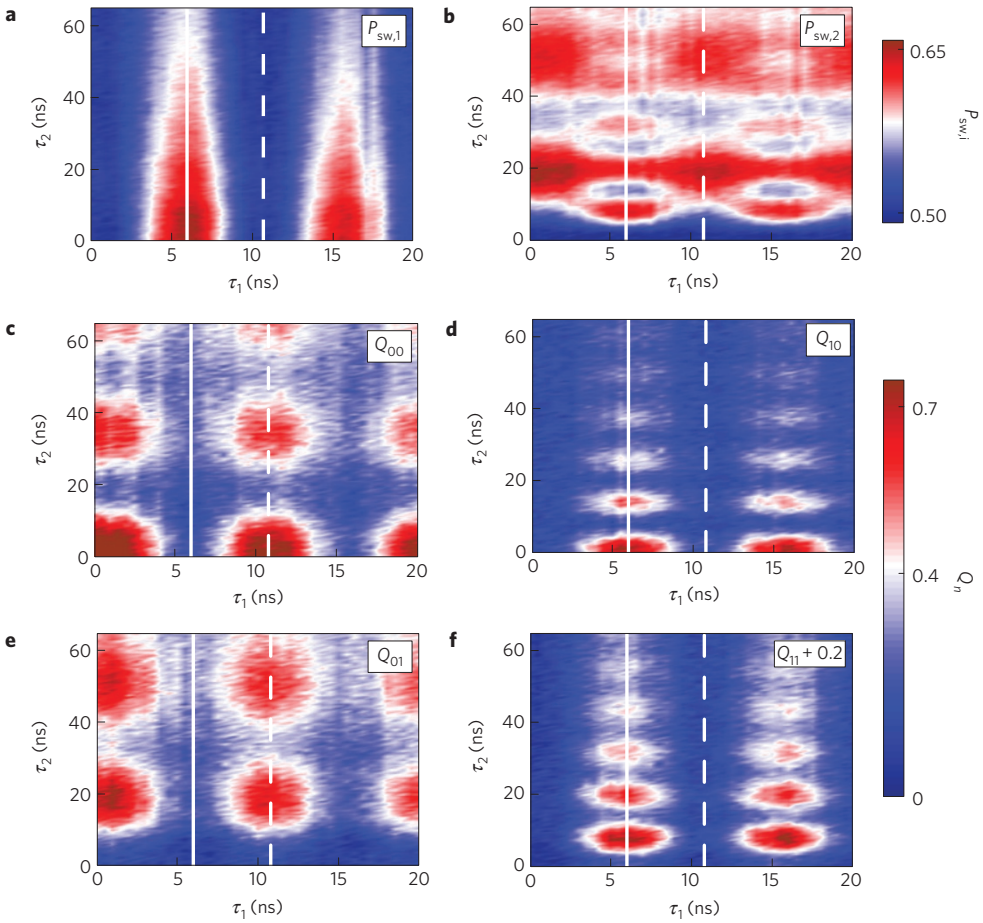

Figure 2 | Driving from a single antenna. Measurement of the state of the qubits, represented by switching probabilities $P_{sw,1}$ and $P_{sw,2}$, after applying a pulse of duration τ_1 resonant with qubit 1, followed by a pulse of duration τ_2 resonant with qubit 2. **a**, $P_{sw,1}$, showing coherent oscillations of qubit 1 induced by pulse 1. The white solid and dashed lines indicate a π- and 2π-rotation respectively. For pulse 2, qubit 1 shows only relaxation. **b**, $P_{sw,2}$, showing coherent oscillations induced by pulse 2. After an odd number of π-rotations on qubit 1, the oscillation frequency is higher than after an even number of π-rotations. For superposition states of qubit 1, a beating pattern of the two oscillations is observed. **c**–**f**, Level occupations Q of the four different levels. Note that a value of 0.2 has been added to Q_{11} to improve visibility.

We consider the class of systems of transversely coupled qubits, described with the Hamiltonian

$$H = -\frac{1}{2}\left(\Delta_1 {\sigma_z}^1 + \Delta_2 {\sigma_z}^2\right) + J {\sigma_x}^1 {\sigma_x}^2 \qquad (1)$$

where Δ_i is the single-qubit energy splitting of qubit i, $\Delta_1 \neq \Delta_2$, J is the qubit–qubit coupling energy and ${\sigma_{x,y,z}}^i$ are the Pauli spin matrices. This Hamiltonian describes many actively used quantum systems[1–6], and often applies for operation at a coherence sweet-spot[3,14,17–19]. The energy levels of this system are shown schematically in Fig. 1b. The arrows indicate the transitions of interest; the blue and red arrows describe the transitions of qubit 1 and 2, respectively. Both pairs are degenerate in frequency, which is typical for transverse coupling. For simplicity, we label the states as if the qubits were uncoupled, although the single-qubit states are mixed by the coupling. This state mixing is central to the method we introduce here. As for all schemes with fixed coupling, the mixing can also lead to a difference between the operational basis and the readout basis. Solutions to this problem depend on the details of the readout scheme. For flux qubits, the readout naturally involves shifting the qubits to a bias position where the problem does not exist.

Our method aims at the selective excitation of a transition of one of the degenerate pairs and is based on simultaneously driving both qubits with the resonance frequency of that pair, employing different amplitudes and phases. The driving is described with the Hamiltonian

$$H_{\mathrm{drive}} = a_1 \cos(\omega t + \varphi_1) {\sigma_x}^1 + a_2 \cos(\omega t + \varphi_2) {\sigma_x}^2 \qquad (2)$$

where ω is the driving frequency and a_i and φ_i are the driving amplitude and phase for qubit i. The transition strength $T_{k\leftrightarrow l} = \langle l|\hat{H}_{\mathrm{drive}}|k\rangle$, with the driving Hamiltonian transformed to an appropriate rotating frame (see Supplementary Information), governs the transition rate and depends on both a_i and φ_i. Figure 1d shows the normalized $|\overline{T}| = |T|/(a_1 + a_2)$ as a function of $a_1/(a_1 + a_2)$, for a fixed phase difference $\varphi_2 - \varphi_1 = 0$. Clearly the two transitions of each qubit generally do not have the same strength T, despite their frequency degeneracy. In addition, for certain settings individual transitions are completely suppressed: the transition is darkened (black dotted lines in Fig. 1d). The darkened transitions provide the desired conditions where one of the two transitions can be excited individually, even though the driving field is resonant with both transitions. The difference in transition strength can be understood intuitively. As coupling leads to mixing of the single-qubit eigenstates, qubit 2 can be excited by driving qubit 1 with a frequency that is resonant with qubit 2. This indirect driving can enhance, counteract and even cancel direct driving of qubit 2. The effect differs for the two degenerate transitions, because the states involved are different superpositions

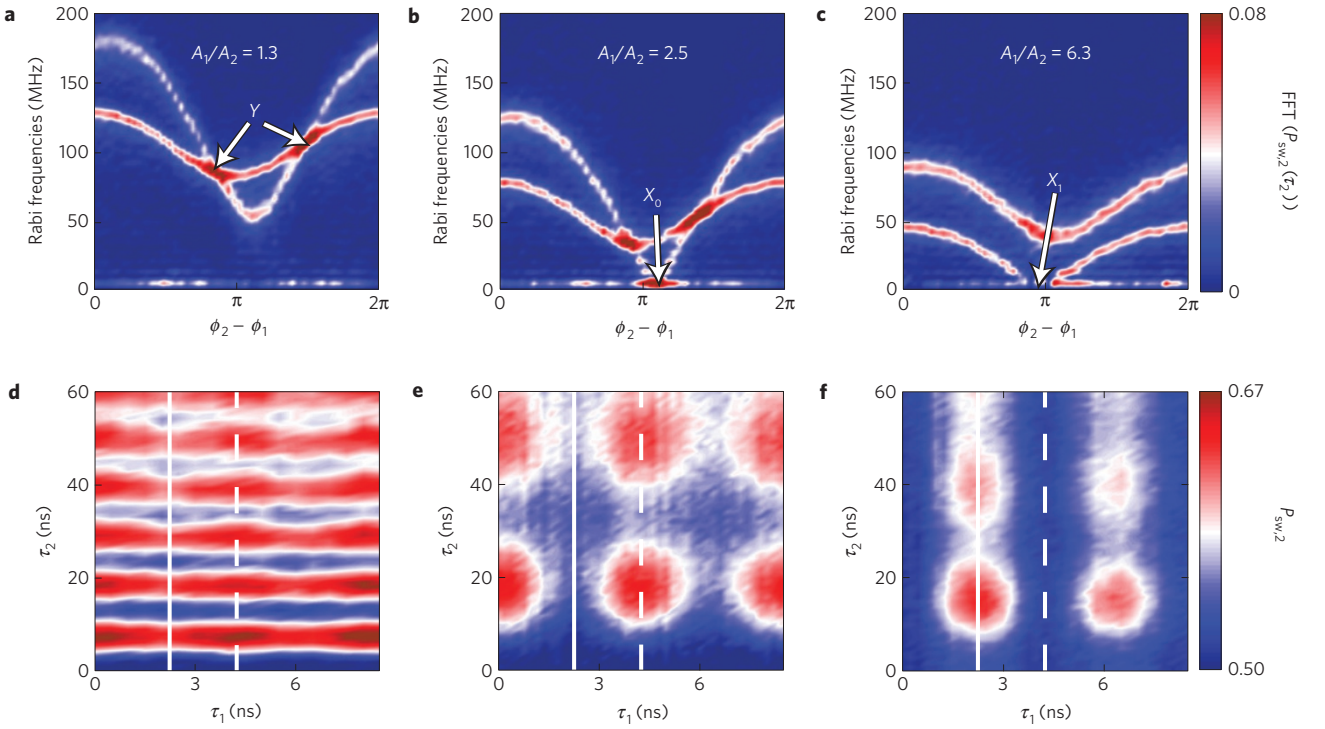

Figure 3 | Transition-strength tuning and darkened transitions. a–c, Rabi frequency dependence on $\phi_2 - \phi_1$ for three different amplitude ratios. The colour scale represents the Fourier component of $P_{sw,2}(\tau_2)$. Qubit 1 is prepared with a $\pi/2$-rotation. Markers X_0 and X_1 indicate the conditions for a darkened transition on 00 ↔ 01 and 10 ↔ 11, respectively. **d–f**, $P_{sw,2}$ versus the durations τ_1 and τ_2. The white solid and dashed lines indicate a π- and 2π-rotation of qubit 1, respectively. The driving conditions are as marked by *Y* left arrow (**d**), X_0 (**e**) and X_1 (**f**).

of the single-qubit eigenstates (see Supplementary Information). For $J \ll |\Delta_1 - \Delta_2|$, and assuming $\Delta_1 > \Delta_2$, one readily finds the driving amplitude ratio

$$\frac{a_2}{a_1} = \frac{J}{\Delta_1 - \Delta_2}$$

which yields $T_{00\leftrightarrow 01} = 0$ for $\varphi_2 - \varphi_1 = 0$ and $T_{10\leftrightarrow 11} = 0$ for $\varphi_2 - \varphi_1 = \pi$. These are the transitions of qubit 2. For the transitions of qubit 1, that is 00 ↔ 10 and 01 ↔ 11, the amplitude ratio is simply inverted. Expressions for arbitrary J are given in the Supplementary Information. Note that for a darkened transition in one qubit, the other is driven more strongly. This non-resonant driving of the other qubit limits the maximum operation frequency. From the usual condition that the transition strength of the unwanted transition should be smaller than its frequency detuning one can derive the maximum operation frequency $4J/h$, which is as fast as any other two-qubit operation.

To experimentally demonstrate this method we employ two coupled flux qubits[1], each consisting of a superconducting loop interrupted by four Josephson tunnel junctions. When biased with a magnetic flux close to half a flux quantum Φ_0, the two states of each qubit are clockwise and anticlockwise persistent-current states. These currents I_p produce opposite magnetic fields, which provides the coupling for the two qubits. Two independent a.c.-operated superconducting quantum interference device magnetometers are used to simultaneously read out the states of the qubits[20,21]. These are switching-type detectors, where the switching probability P_{sw} is a measure for the magnetic field. At a bias of $\Phi_0/2$ the system is described by the Hamiltonian of equation (1). Here the eigenstates of each qubit are symmetric and antisymmetric superpositions of the two persistent-current states, with level separation Δ. The device is shown in Fig. 1a. The qubits are characterized by the persistent currents $I_{p,1} = 355$ nA and $I_{p,2} = 460$ nA and the energy splittings $\Delta_1/h = 7.88$ GHz and $\Delta_2/h = 4.89$ GHz. The qubit–qubit coupling strength is $2J/h = 410$ MHz.

For our fabricated quantum objects the spatial locations are well defined, and the individual control of amplitude and phase for each qubit according to equation (2) can be easily achieved using local magnetic fields. We employ two on-chip antennas, indicated as A_1 and A_2 in Fig. 1a, both coupling to both qubits, with a stronger coupling to the closer one. Driving the two qubits from both antennas is described with

$$H_{\text{drive}} = A_1 \cos(\omega t + \phi_1)(m_{11}\sigma_x{}^1 + m_{12}\sigma_x{}^2) + A_2 \cos(\omega t + \phi_2)(m_{21}\sigma_x{}^1 + m_{22}\sigma_x{}^2)$$

where A_j and ϕ_j are the driving amplitude and phase for antenna j and m_{ji} is the coupling of antenna j to qubit i. Note that any combination of a_i and φ_i in equation (2) can be achieved with the proper choice of A_j and ϕ_j. For this device $m_{12}/m_{11} = 0.32$, $m_{21}/m_{22} = 0.33$ and $m_{11} = m_{22}$.

For the experimental demonstration we choose to focus on the degenerate transitions of qubit 2. We first show that, if the qubits are driven from a single antenna, the two degenerate transitions exhibit a different Rabi frequency. We apply two pulses on antenna 1: the first pulse is resonant with qubit 1; the second pulse is resonant with qubit 2. Figure 1c shows a schematic of the pulse sequence; note that here $A_2 = 0$. The experiment is repeated for varying durations τ_1 and τ_2 of pulses 1 and 2. The switching probability $P_{sw,1}$ of detector 1 is depicted in Fig. 2a, showing a few Rabi oscillation periods as a function of the pulse duration τ_1. Varying τ_2 does not lead to oscillations of qubit 1, as pulse 2 is non-resonant, and only relaxation is observed. The oscillations of qubit 2, induced by the second pulse, are visible in $P_{sw,2}$ (Fig. 2b). Here we distinguish two oscillation frequencies. Along the white solid line, where qubit 1 is prepared in the excited state, qubit 2 oscillates with a Rabi frequency

of 85 MHz. For qubit 1 prepared in the ground state, along the white dashed line, the Rabi frequency $f = 31$ MHz of qubit 2 is lower. For qubit 1 in a superposition of the ground and excited states, qubit 2 shows a beating pattern of both oscillations.

A more detailed analysis allows us to unravel the two frequencies of Fig. 2b and determine which levels are participating in each of the oscillations. We extract the level occupations Q_{00}, Q_{01}, Q_{10} and Q_{11} from the individual switching probabilities (see Supplementary Information). The result is shown in Fig. 2c–f. After an odd number of π-rotations of qubit 1, there are oscillations only between states 10 and 11, not for states 00 and 01. After an even number of π-rotations of qubit 1 the situation is reversed; now the states 00 and 01 oscillate. The two oscillation frequencies are clearly linked to the two different transitions.

To demonstrate the tunability of the transition strengths we drive both antennas simultaneously, using the same frequency and controlling independently the amplitudes A_1, A_2 and phases ϕ_1, ϕ_2. In this two-pulse experiment (Fig. 1c), the first pulse prepares qubit 1 with a $\pi/2$-rotation and the duration τ_2 of the second pulse is varied. As qubit 1 is in a superposition state, both Rabi frequencies are present in the dynamics of qubit 2. In Fig. 3a–c we show the Fourier transform for the measured oscillations. Each graph is measured with a different amplitude ratio A_1/A_2, with fixed phase $\phi_1 = 0$ and varying ϕ_2. Figure 3a, with $A_1/A_2 = 1.3$, shows a typical result for an arbitrary amplitude ratio; the Rabi oscillation frequencies of both transitions clearly depend on $\phi_2 - \phi_1$, but nowhere is a transition darkened. Note the occurrence of equal Rabi frequencies for two phase conditions, as denoted by Y. For $A_1/A_2 = 2.5$ in Fig. 3b we observe that for $\phi_2 - \phi_1 \approx \pi$ (indicated by X_0) the transition $10 \leftrightarrow 11$ is fully darkened, whereas the $00 \leftrightarrow 01$ transition shows a non-zero oscillation frequency. In Fig. 3c with $A_1/A_2 = 6.3$ the situation is reversed, with the $00 \leftrightarrow 01$ transition being suppressed (denoted by X_1). This clearly demonstrates our method, as we selectively excite one of two transitions, despite their frequency degeneracy. Calculations of T are in good agreement with the experimental results, provided we allow for different transmissions of amplitudes and phases of the antennas to the qubits, which we attribute to the influence of the detector circuits.

To further investigate the special cases of equal Rabi frequencies (Y), and darkened transitions (X_0, X_1), we again vary the durations τ_1 and τ_2, using both antennas for the second pulse. The results should be compared with Fig. 2b. Figure 3d shows $P_{\mathrm{sw},2}$ for driving conditions denoted by Y (left arrow): the oscillation frequency of qubit 2 does not depend on the state of qubit 1. For the conditions marked by X_0, we observe oscillations of qubit 2 only when qubit 1 is in the ground state, as shown in Fig. 3e. Similarly for the conditions marked by X_1, now we observe oscillations of qubit 2 only if qubit 1 is in the excited state (Fig. 3f).

The demonstrated capability to selectively manipulate transition strengths in frequency-degenerate transitions has important applications. A π-pulse using condition X_1 or X_0 provides a 1-controlled- and 0-controlled-NOT gate, respectively. This enables certain systems, including the flux qubit used here, to be fully operated at the coherence-optimal point, without level shifting by either d.c. or strong a.c. signals. Note that the use of extra coupling elements is neither required nor prohibited. If extra coupling elements are used, our method can replace more complicated schemes. For conditions similar to Y, taking care of the individual rotation angles, also single-qubit gates can be implemented. The controlled-NOT and single-qubit gates together form a universal set, implying that our method fulfils all requirements for constructing any single- or two-qubit gate. Up to small errors, the method also scales to three or more qubits with transverse coupling. Detailed calculations will be presented elsewhere.

We have introduced and experimentally demonstrated a method to control transition strengths by applying a non-uniform driving field. Darkened transitions are created and employed for the selective excitation of degenerate transitions. As this method improves the simplicity and coherence conditions for operations in a variety of quantum systems, the prospect of carrying out large-scale quantum algorithms is enhanced significantly.

Received 17 March 2010; accepted 18 June 2010; published online 1 August 2010

References

1. Mooij, J. E. *et al.* Josephson persistent-current qubit. *Science* **285,** 1036–1039 (1999).
2. Nakamura, Y., Pashkin, Y. A. & Tsai, J. S. Coherent control of macroscopic quantum states in a single-cooper-pair box. *Nature* **398,** 786–788 (1999).
3. Vion, D. *et al.* Manipulating the quantum state of an electrical circuit. *Science* **296,** 886–889 (2006).
4. Martinis, J. M., Nam, S., Aumentado, J. & Urbina, C. Rabi oscillations in a large Josephson-junction qubit. *Phys. Rev. Lett* **89,** 117901 (2002).
5. Schreier, J. A. *et al.* Suppressing charge noise decoherence in superconducting charge qubits. *Phys. Rev. B* **77,** 180502 (2008).
6. Manucharyan, V. E., Koch, J., Glazman, L. I. & Devoret, M. H. Fluxonium: Single cooper-pair circuit free of charge offsets. *Science* **326,** 113–116 (2009).
7. Linden, N., Barjat, H. & Freeman, R. An implementation of the Deutsch-Jozsa algorithm on a three-qubit NMR quantum computer. *Chem. Phys. Lett.* **296,** 61–67 (1998).
8. Plantenberg, J. H., de Groot, P. C., Harmans, C. J. P. M. & Mooij, J. E. Demonstration of controlled-NOT quantum gates on a pair of superconducting quantum bits. *Nature* **447,** 836–839 (2007).
9. Jones, J. A. & Knill, E. Efficient refocusing of one-spin and two-spin interactions for NMR quantum computation. *J. Magn. Reson.* **141,** 322–325 (1999).
10. Paraoanu, G. S. Microwave-induced coupling of superconducting qubits. *Phys. Rev. B* **74,** 140504 (2006).
11. Niskanen, A. O. *et al.* Quantum coherent tunable coupling of superconducting qubits. *Science* **316,** 723–726 (2007).
12. Sillanpää, M. A., Park, J. I. & Simmonds, W. Coherent quantum state storage and transfer between two phase qubits via a resonant cavity. *Nature* **449,** 438–442 (2007).
13. McDermott, R. *et al.* Simultaneous state measurement of coupled Josephson phase qubits. *Science* **307,** 1299–1302 (2005).
14. Rigetti, C., Blais, A. & Devoret, M. Protocol for universal gates in optimally biased superconducting qubits. *Phys. Rev. Lett.* **94,** 240502 (2005).
15. Majer, J. *et al.* Coupling superconducting qubits via a cavity bus. *Nature* **449,** 443–447 (2007).
16. Simmonds, R. W. *et al.* Decoherence in Josephson phase qubits from junction resonators. *Phys. Rev. Lett.* **93,** 077003 (2004).
17. Yoshihara, F., Harrabi, K., Niskanen, A. O., Nakamura, Y. & Tsai, J. S. Decoherence of flux qubits due to $1/f$ flux noise. *Phys. Rev. Lett.* **97,** 167001 (2006).
18. Liu, Y-x., Wei, L. F., Tsai, J. S. & Nori, F. Controllable coupling between flux qubits. *Phys. Rev. Lett.* **96,** 067003 (2006).
19. Bertet, P., Harmans, C. J. P. M. & Mooij, J. E. Parametric coupling for superconducting qubits. *Phys. Rev. B* **73,** 064512 (2006).
20. Lupaşcu, A. *et al.* Quantum non-demolition measurement of a superconducting two-level system. *Nature Phys.* **3,** 119–125 (2007).
21. de Groot, P. C. *et al.* Low-crosstalk bifurcation detectors for coupled flux qubits. *Appl. Phys. Lett.* **96,** 123508 (2010).

Acknowledgements

We acknowledge L. M. K. Vandersypen, G. A. Steele, I. T. Vink, J. Baugh and the Delft Flux Qubit Team for help and discussions and A. van der Enden, R. G. Roeleveld, B. P. van Oossanen and the Nanofacility for technical and fabrication support. This work is supported by NanoNed, FOM, NSERC Discovery and EU projects EuroSQIP and CORNER.

Author contributions

P.C.d.G. and A.L. devised the method. P.C.d.G. designed the experiment, and designed and fabricated the sample. P.C.d.G. and J.L. carried out the experiments and analysed the data. S.A. analysed the method theoretically. R.N.S. developed and provided dedicated electronics. P.C.d.G., J.E.M. and C.J.P.M.H. wrote the manuscript. J.E.M. and C.J.P.M.H. supervised the project.

Additional information

The authors declare no competing financial interests. Supplementary information accompanies this paper on www.nature.com/naturephysics. Reprints and permissions information is available online at http://npg.nature.com/reprintsandpermissions. Correspondence and requests for materials should be addressed to P.C.d.G.